C. R. Physique 15 (2014) 258–268

Contents lists available at ScienceDirect

Comptes Rendus Physique

www.sciencedirect.com

Electron microscopy / Microscopie électronique

Using electron beams to investigate catalytic materials

Apports de la microscopie électronique à l'étude des matériaux catalytiques

Bingsen Zhang [a], Dang Sheng Su [a,b,*]

[a] *Shenyang National Laboratory for Materials Science, Institute of Metal Research, Chinese Academy of Sciences, 72 Wenhua Road, Shenyang 110016, China*
[b] *Department of Inorganic Chemistry, Fritz Haber Institute of the Max Planck Society, Faradayweg 4–6, 14195 Berlin, Germany*

ARTICLE INFO

Article history:
Available online 28 January 2014

Keywords:
Electron microscopy
Catalyst
Chemical composition
Surface
Dynamic process
Particle shape

Mots-clés :
Microscopie électronique
Catalyseur
Composition chimique
Surface
Processus dynamique
Forme des particules

ABSTRACT

Electron microscopy (EM) enables us, not only to reveal the morphology, but also to provide structural, chemical and electronic information about solid catalysts at the atomic level, providing a dramatic driving force for the development of heterogeneous catalysis. Almost all catalytic materials have been studied with EM in order to obtain information about their structures, which can help us to establish the synthesis–structure–property relationships and to design catalysts with new structures and desired properties. Herein, several examples will be reviewed to illustrate the investigation of catalytic materials by using electron beams.

RÉSUMÉ

Le microscope électronique à transmission (TEM) permet, non seulement de révéler la morphologie, mais aussi d'apporter des informations à l'échelle atomique sur les propriétés structurales, chimiques et électroniques de catalyseurs solides. Ceci en fait un outil majeur dans le développement de la catalyse hétérogène. Presque tous les matériaux catalytiques ont été étudiés par TEM afin de caractériser leur structure, ce qui aide considérablement à la recherche des relations synthèse–structure–propriétés, ainsi qu'à la production de nouveaux matériaux aux propriétés ciblées. Dans cette revue, plusieurs exemples ont été sélectionnés pour illustrer les méthodes et les résultats de l'étude des matériaux catalytiques, lorsque le faisceau d'électrons d'un TEM est utilisé comme faisceau sonde.

1. Introduction

Catalysis is central to the production of fuels and chemicals, including more than 70% of today's chemical products [1,2]. Nowadays, developing new catalyst with high activity, selectivity and stability constitutes an enormous challenge. Furthermore, it must be realized under sustainable conditions: the main constituents of new catalysts must be abundant in nature, cheap, and their production process must be environmentally friendly. Most importantly, new catalysts must be developed for processes that are not possible today such as artificial photosynthesis or hydrogen production from water. These new challenges for materials science and catalysis are seen as one of the major driving forces for the current revolution in

* Corresponding author at: Shenyang National Laboratory for Materials Science, Institute of Metal Research, Chinese Academy of Sciences, 72 Wenhua Road, Shenyang 110016, China.
E-mail address: dangsheng@fhi-berlin.mpg.de (D.S. Su).

1631-0705/$ – see front matter
http://dx.doi.org/10.1016/j.crhy.2013.11.001

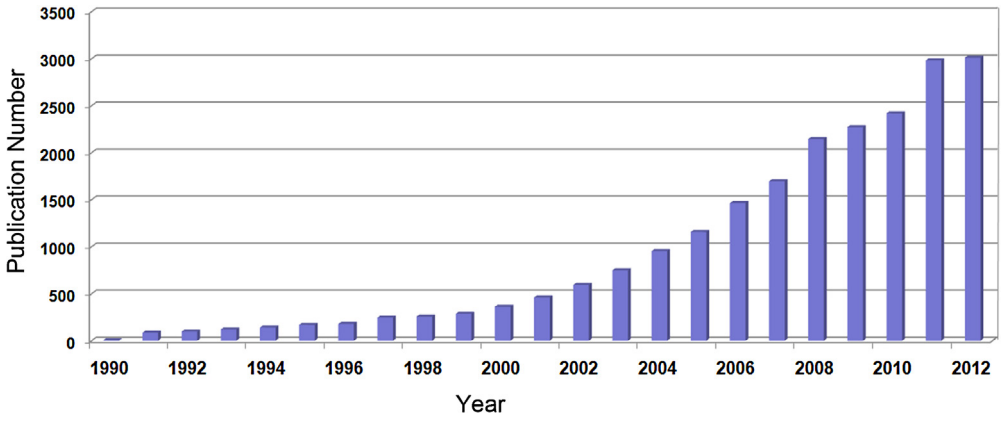

Fig. 1. The number of papers on catalysts investigated by TEM published annually, from 1990 to 2012. (Data from ISI Web of knowledge on February 10, 2013.)

electron microscopy. Apart from nanoscience and nanotechnology, catalysis is one of the most important areas, where EM, specially TEM and STEM, have found their applications [3–23]. It can be said that the evolution of catalysis science is based on the ability to cope with the structural complexity of solid catalysts, which is largely made possible by the advancement of electron microscopy [24,25]. Fig. 1 shows the number of papers on solid catalysts investigated by TEM annually from 1990 to 2012 as reported by ISI Web of Science. The spectacular rise in the annual total of papers clearly indicates that TEM and its associated techniques have significantly contributed to the investigation in the field of solid catalysts.

This article focuses on the applications of advanced TEM techniques to the fundamental study of solid catalysts. Herein, we will only show some selected examples due to the offered limited space. They have been selected to demonstrate how different forms of advanced TEM can be used to investigate solid catalysts. It is expected that better understanding of the nature of the solid catalyst in chemical reactions can help to design and develop catalysts with tailored properties.

2. TEM investigation of catalytic materials

Many characterization tools are widely used to analyze solid catalysts, such as X-ray diffraction (XRD), X-ray photoelectron spectroscopy (XPS), Raman spectroscopy, and so on. All these powerful tools, however, do not exhibit high spatial resolution. Scanning probe microscopes can provide images of a flat surface with a spatial resolution equivalent to that of a TEM/STEM. But they require a special treatment of the surface in many cases, and sometimes the application is limited; e.g., scanning tunneling microscope cannot image the surface of an insulator. TEM/STEM is not simply a complementary tool of the aforementioned methods. As we will see below, it has become a quite robust and versatile tool for catalysis research. It provides essential information (both static and dynamic) on solid catalysts, which cannot be obtained with any other characterization method [26,27].

2.1. Determination of the chemical composition of catalysts (EDS—Energy-Dispersive X-ray Spectroscopy—and EELS—Electron Energy-Loss Spectroscopy)

In many cases, revealing the elemental distribution in a catalyst or tracing the elements in a catalytic reaction is crucial for probing phase composition, understanding chemical processes, and detecting the growth history of the reaction-driven intermediates. Therefore, it is of paramount importance to reveal the composition distribution for the design of catalytic nanomaterials and for unraveling the catalytic mechanism that is involved [28–31]. EDS is a standard technique on a modern TEM for qualitative and quantitative elemental analysis, which is suitable for heavy elements with high fluorescence yield [32–34]. On the other hand, the use of core-level EELS spectroscopy is more suited to the analysis of light elements, such as boron, carbon, nitrogen, oxygen, and phosphorus [35–37]. Both EDS and EELS analysis can be carried out with very high resolution, allowing chemical analysis of individual nanoparticles (NPs) across surfaces or in interfacial areas [38–42].

EDS elemental maps are suitable for mapping the composition of metal or metal oxide nanomaterials, especially bi- or multi-metallic NPs, such as AuPd catalysts [34]. An experiment using physically mixed Au/AC and Pd/AC (AC = activated carbon) as the catalyst has been designed in the liquid-phase oxidation of benzyl alcohol by aerobic oxygen. The evolution of the physically mixed catalyst structures at different stages in the catalytic reaction was studied by spatially resolved elemental mapping techniques. Fig. 2 shows the results of EDS spectrum imaging on a few particles from one piece of original Au/AC in the physically mixed catalyst after 0.5 h of reaction. It includes the HAADF–STEM image, Au and Pd maps and the two maps superimposed. The integrated spectrum of all the pixels in the scanned area is shown in Fig. 2(b). It clearly indicates the migration of Pd atoms onto the Au particles, thereby forming bimetallic particles. The quantitative

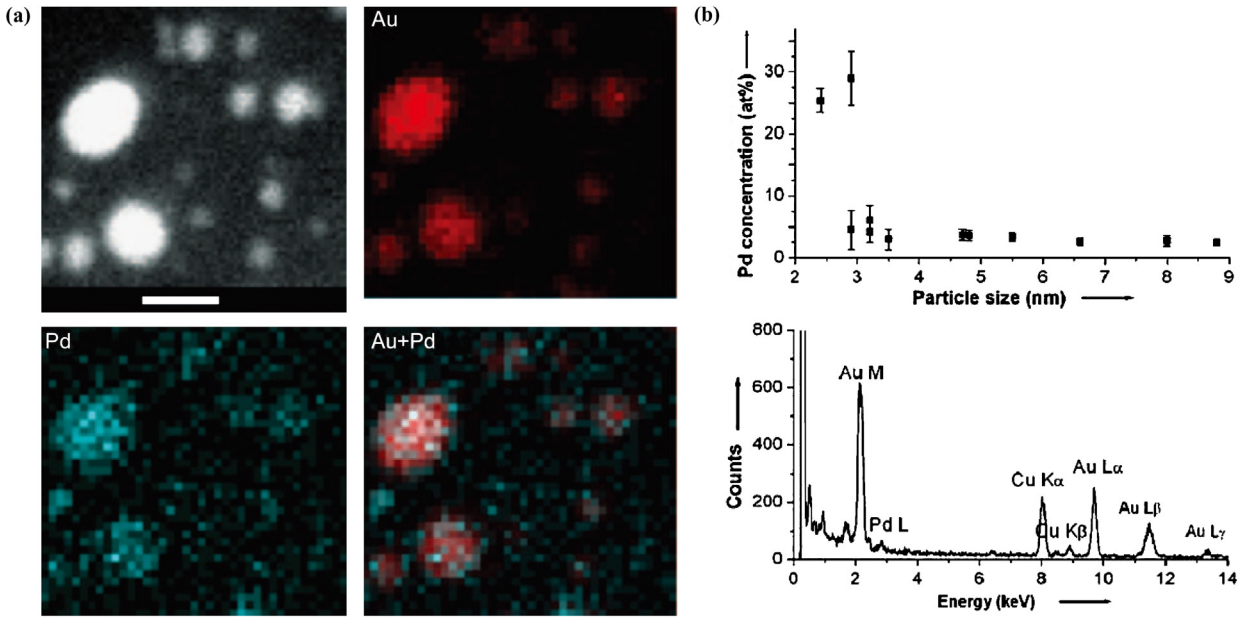

Fig. 2. (Color online.) (a) High-Angle Annular Dark Field (HAADF)–STEM image, Au and Pd maps and the two superimposed maps from one specimen of original Au/AC in the physically mixed catalyst after 0.5 h of benzyl alcohol oxidation. (b) Pd concentration of the particles as a function of the particle size from map (a) and other maps on the same sample (top), and integrated EDS spectrum from the whole scanned region in map (a). Scale bar in HAADF–STEM image is 10 nm. Reprinted with permission from [34], copyright (2010) Wiley-VCH Verlag GmbH & Co. KGaA, Weinheim, Germany.

analysis of the integrated spectrum using Au L and Pd L excitations suggests an Au/Pd atomic ratio of 96.6 : 3.4. The quantification results are plotted in Fig. 2(b) as well. For the mixed catalyst after 30 min of reaction, the Pd concentration is much higher for the particle smaller than 3 nm. It is quite understandable that at the beginning the same deposition rate of Pd will lead to a high Pd ratio on extra-small particles. In this case, therefore, the elemental distribution can be traced by EDS in synthesis and reaction, and then related to the performance in the liquid-phase oxidation of alcohols.

Energy-filtered TEM (EFTEM) is the preferred method to give two-dimensional images of the light elements' distribution. This is not only due to the physics of the signal generation process, but also to the EELS' relatively high geometrical signal collection efficiency relative to that encountered with EDS. Fig. 3 shows the elemental distribution in the modified-ordered mesoporous carbons (OMCs), which confirms that the B and O functionalities are homogeneously distributed in the carbonaceous framework [43]. In addition, since no specific procedure was carried out to get rid of the involved salt species, sodium was also supposed to exist in the resultant materials. However, the Na element is not easily detected by EELS at low concentrations because its characteristic edges lie either at low energy values (30 eV for Na-2p) or at high ones (1080 eV for Na-1s). Alternately, the Na presence can easily be confirmed by its EDS signal. Therefore, from the combination of the EDS and EELS mapping, it is well confirmed that the B, C, O, Na are homogeneously distributed in the B-modified-OMC matrix, which constitutes a promising electrode material for supercapacitors.

2.2. Surface of a real catalyst

Since the catalytic reactions occur at the surface of a catalyst, its structure becomes essential to understanding the reaction mechanisms. Usually, the surface structure of a catalyst is studied by surface techniques (e.g., AFM, STM, and PEEM) on model catalyst systems under very high-vacuum conditions [26]. With the development of spherical aberration-corrected TEMs, the delocalization effects that mask the visibility of the detailed surface perimeter are strongly reduced so that the atomic structure of a catalyst surface is clearly visible. Thereafter, the active sites on industrial catalysts and the surface redox dynamics under near-reaction conditions at high temperature can nowadays be investigated by aberration-corrected TEM.

For instance, silver catalysts are used in many chemical reactions, such as hydrogenation of unsaturated aldehydes, partial oxidation of methanol to formaldehyde and oxidative coupling of methane to ethane and ethylene. In the 1990s, Ertl et al. identified the presence of surface and subsurface oxygen atoms on and in Ag catalysts by spectroscopy methods [44,45], which was quite meaningful for understanding the catalytic reaction steps and mechanisms of silver catalysts. However, the exact location of these surface and subsurface oxygen atoms has remained an unanswered question in Ag catalysis, until aberration-corrected TEM observations have revealed the surface structure of real industrial Ag catalysts [46]: surface features, such as terraces, kinks, and edges can clearly be visualized and investigated, as shown in Fig. 4.

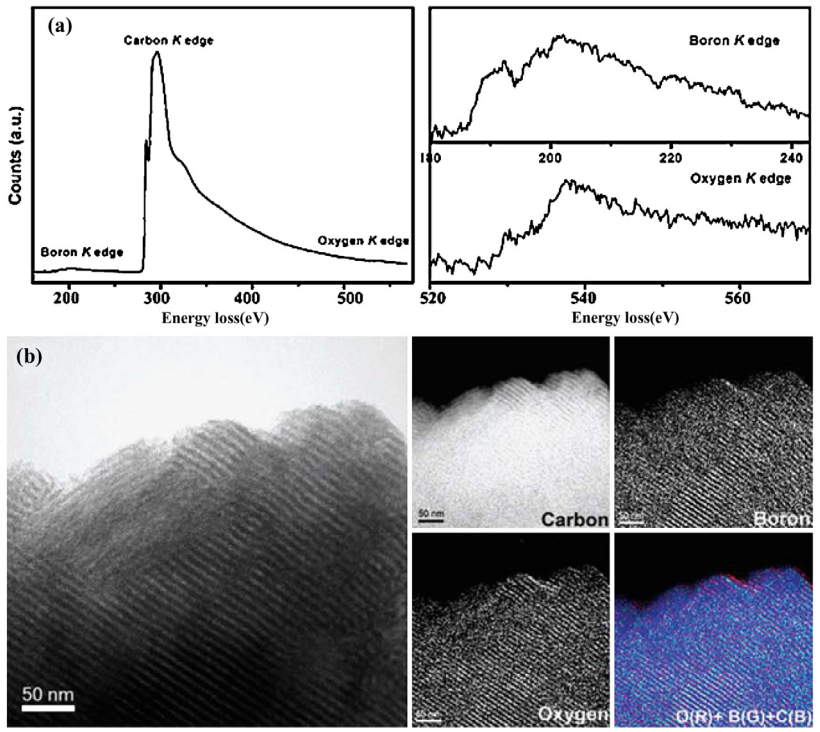

Fig. 3. (Color online.) (a) EELS spectra. (b) EFTEM: zero loss bright field image, C, B, O energy filtered images and their colored combination (C—blue, B—green, and O—red). For interpretation of references to color, see the online version of this article. Reprinted with permission from [43], copyright (2013) The Royal Society of Chemistry.

2.3. Supported catalysts

Among heterogeneous catalysts, supported catalysts play a pivotal role in many practical processes for the sustainable production of fuels and chemicals [5,47–49]. For understanding the catalytic performance of a supported catalyst, it is crucial to have access to a broad range of complementary information, such as particle size distribution (PSD), spatial dispersion, NP shape, 3D structure, metal–support interaction, and identification of single metal atoms and clusters. We will now demonstrate through a selection of practical examples how the modern TEM capabilities can bring answers to these questions.

2.3.1. Identification of single metal atoms and clusters

One of the most important achievements obtained in catalysis by using electron microscopy is the observation of individual atoms, metal atoms and clusters on supported catalysts and the assignment of their possible role in catalysis. With the development of aberration-corrected STEM, interesting results concerning the active centers of real catalyst have been reported. The "single-atom" Pt/FeO_x catalysts consist only of isolated single Pt atoms anchored to the surfaces of iron oxide nanocrystallites: it has been clearly revealed by atomic resolution HAADF–STEM that these Pt atoms (white circles) occupy exactly the positions of the Fe atoms [50], as shown in Fig. 5. In addition, the analysis of images obtained sequentially by varying the beam focus setting shows that all observed individual Pt atoms are located either on the surfaces or in the near subsurfaces of the FeO_x. This catalyst exhibits extremely high atom efficiency, excellent stability and high activity for both CO oxidation and preferential oxidation of CO in H_2 [50].

2.3.2. Particle size distribution of supported catalysts

It is well known that the performance of a catalyst greatly depends on its dimensions or size. In many cases, tiny clusters and even single atoms (see Fig. 5) on a support have been identified as the main active sites for catalysis. Therefore, an accurate particle size distribution (PSD) of the catalysts is very important for understanding the involved catalysis mechanisms, which guarantee their effective application in the chemical industry [48,51].

Among the methods for measuring PSDs, HRTEM may be the most popular one in the case of small particles, owing to its direct visibility and accessibility. A prerequisite for a meaningful PSD is that all particles with sizes ranging from small ($<$2 nm) to large ($>$20 nm) are imaged and counted, and that the size (diameter) of the particles can be measured precisely on the digital images. As the PSD calculated by HRTEM may be inaccurate, HAADF–STEM imaging is a rich alternative in many cases [48,51]. Fig. 6 shows typical pairs of HRTEM and HAADF–STEM images of Ru NPs supported on carbon (Fig. 6(a)–(b)) and of Pd NPs supported on iron oxides (Fig. 6(c)–(d)). It is obvious that the smaller particles are only visible

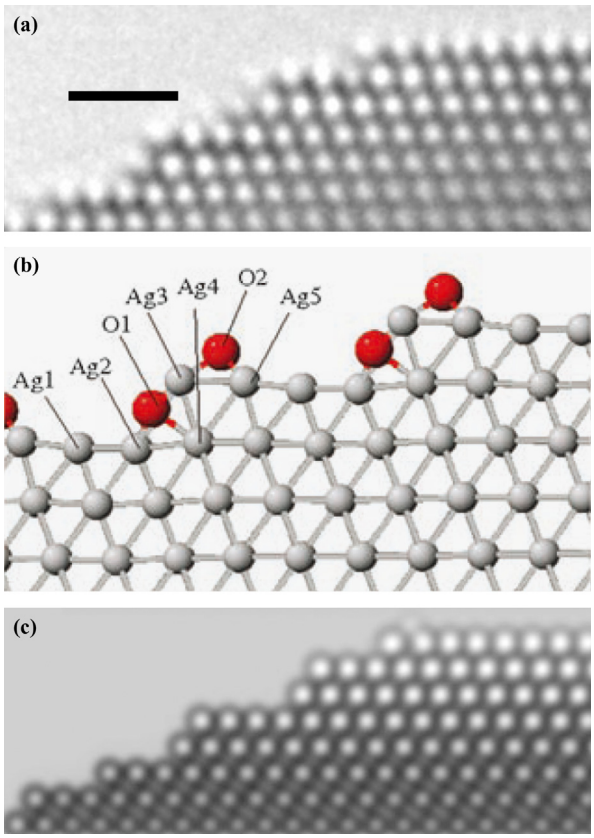

Fig. 4. (Color online.) (a) An experimental high-resolution image of Ag catalyst. (b) Structural model obtained from DFT calculations showing the position of subsurface (O1) and surface (O2) oxygen of the surface of Ag and (c) a simulated high-resolution image using the structure of (b). DFT calculations were based on the HRTEM observations showing a more realistic silver surface consisting of steps and terraces, and identified two distinct kinds of oxygen atoms, one adsorbed on the step edge (O2) and the other in the step edge (O1). Reprinted with permission from [46], copyright (2008) Wiley-VCH Verlag GmbH & Co. KGaA, Weinheim, Germany.

in the STEM images, but not in the HRTEM ones, in particular for Pd NPs supported on FeO_x. Over the same regions exactly, the obtained numbers of particles within a given size window is much larger in HAADF–STEM mode, in particular for the smaller sizes. Furthermore, the lower numbers deduced from the HRTEM images can introduce aliasing effects and lead to inaccurate PSD estimations, such as the so-called multimodal distribution suggested by this study. Therefore, the PSD information provided by the STEM is generally more accurate, which is crucial towards a full understanding of the catalytic performance of supported metal catalysts. Finally, the determination of mean PSD should be complementarily checked with the support of XRD and gas chemisorption measurements [48,51,52].

2.3.3. Spatial distribution of NPs on supports

For understanding the catalytic performance of a supported catalyst, not only the PSD of the NPs, but also their spatial distribution is of importance. For instance, when mesoporous materials (silica, titania, and carbon) or carbon nanotubes (CNTs) are used as supports, the exact location of the supported metal or metal oxide NPs must be determined. However, the routine methods such as HRTEM or STEM imaging do not provide the whole spatial distribution of NPs, because they only generate two-dimensional (2D) projections of a three-dimensional (3D) structure. It is not obvious to deduce the real 3D structure from 2D TEM images. Sometimes, simple tricks can give 3D information, such as tilting the specimen in a TEM, which produces images of the same region viewed with different perspectives, delivering reliable information on the location of the NPs, for instance inside or outside CNTs [53]. However, this method cannot be applied to many situations.

Electron tomography (ET) has been extensively developed over the past years (see the contribution by S. Bals in the present issue). It has become the most general and efficient method to reconstruct the 3D structure of nano-objects from a tilt series of 2D images, and it has consequently been used fruitfully for a number of solid catalysts [10,18,56–60]. As an example, Fig. 7(a) shows a surface render of a reconstructed electron tomogram of bimetallic Pt–Ru particles supported on and within a disordered mesoporous silica catalyst [54]. The high loading of particles within the catalyst structure is clearly visible, with the true 3D nature of the reconstructed data and of the pore network fully appreciated. In another example, Au nanocatalysts on titania show a propensity to reside in crevices between the individual titania grains, as shown in Fig. 7(b)–(c) [55]. In the field of catalysis, ET is definitely a powerful approach, in particular for revealing the spatial

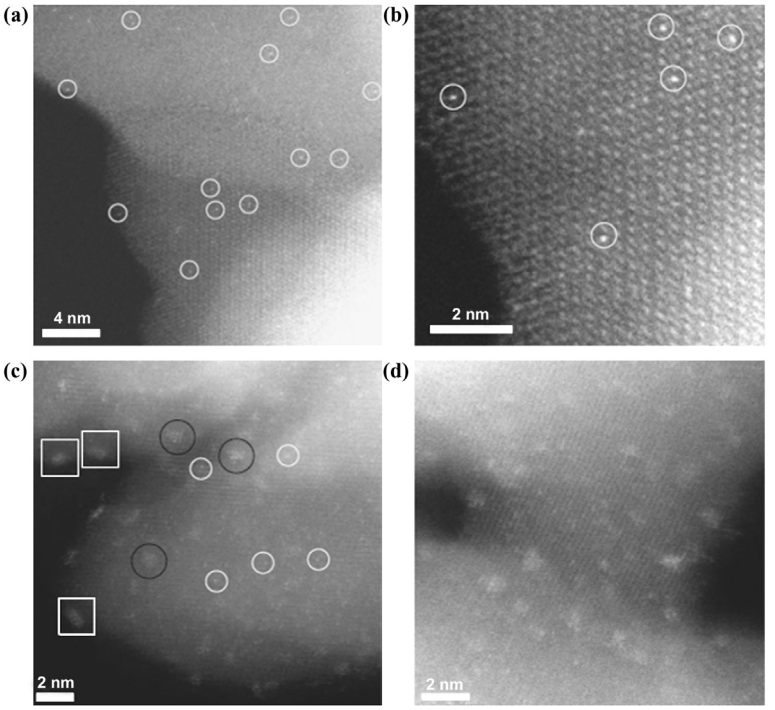

Fig. 5. HAADF–STEM images of samples A (the single-atom Pt_1/FeO_x catalyst with a Pt/Fe atomic ratio of 1/1430 and a Pt loading of 0.17 wt%) and B (a similar catalyst with a Pt/Fe atomic ratio of 1/95 and a Pt loading of 2.5 wt%). (a), (b): In sample A, Pt single atoms (white circles) are seen to be uniformly dispersed on the FeO_x support (a) and occupy exactly the positions of the Fe atoms (b). Examination of different regions reveals that only Pt single atoms are present in sample A. (c), (d): In sample B, a mixture of single atoms (white circles), two-dimensional Pt rafts consisting of fewer than 10 Pt atoms (black circles) and three-dimensional Pt clusters of size about 1 nm or less (white squares) are observed clearly. Reprinted with permission from [50], copyright (2011) Nature Publishing Group.

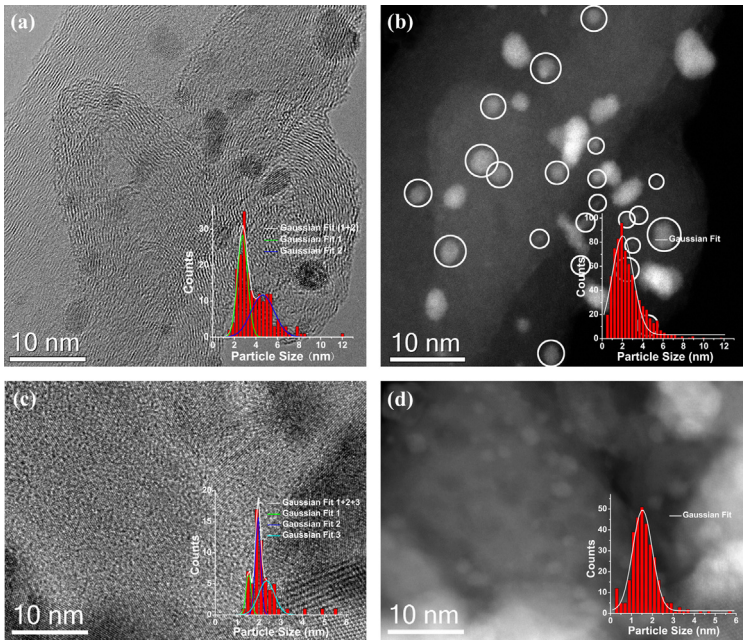

Fig. 6. (Color online.) A typical pair of (a) HRTEM and (b) HAADF–STEM images of Ru NPs supported on CNT, and a typical pair of (c) HRTEM and (d) HAADF–STEM images of Pd NPs supported on FeO_x. The insets are the corresponding PSD. The smaller particles (circled in (b)) are not visible on HRTEM image (a); most Pd NPs are invisible in (c), whereas they are distinctly revealed in (d). Reprinted with permission from [51], copyright (2012) John Wiley & Sons Ltd.

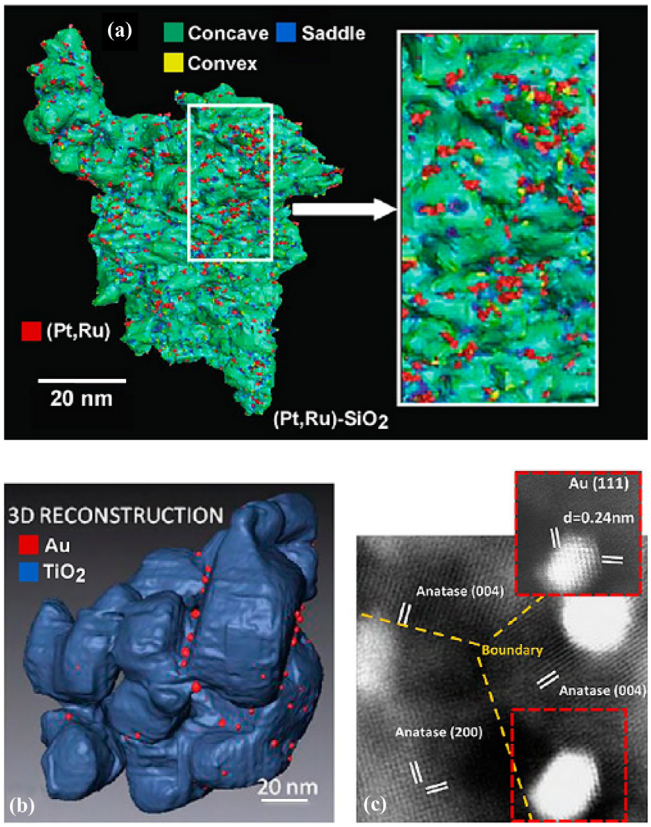

Fig. 7. (Color online.) (a) ET reconstruction of (Pt, Ru) nanocatalysts supported on a disordered mesoporous silica substrate. The surface-rendered visualization of the silica support has been color-coded according to the local Gaussian curvature. The nanocatalysts (red) appear to prefer to anchor themselves at the (blue) saddle-points [54]. (b) Surface-rendered visualization of an ET reconstruction of Au nanocatalysts (red) supported on titania (blue). The nanocatalysts are located in the crevices between titania crystallites; confirmed by the AC–STEM image in panel (c) [55]. For interpretation of references to color, see the online version of this article. Reprinted with permission from [56], copyright (2012) The American Chemical Society.

distribution of NPs on supports. In a few selected cases, the resolution of ET has recently reached the atomic level [57, 61–64].

2.3.4. Shapes of supported metal NPs

Metal NPs exhibiting fascinating optical, electronic, magnetic, and chemical properties that are often radically different from their bulk counterparts, have received wide recognition [49]. One major feature is their high number of surface atoms, which increases with the decrease of particle size, and these surface atoms are among the most active sites in catalysis [65]. Surface atoms located at the edges or in the corners are yet more active than those in planes, and their number also increases with the decrease of the particle size [65]. As the number of surface atoms present in NPs governs their catalytic reactivity, the most detailed knowledge of their shape and size is of prime importance. Spherical aberration-corrected TEMs can now reveal with atomic resolution the local and surface structure of these metal nanoparticles.

Fig. 8 shows the structure evolution of twinned Ru NPs supported on carbon nanotubes (CNTs) rearranging into Ru single nanocrystals under microwave irradiation. Many multiply twinned Ru NPs that consist of several subunits are still visible in the samples after both 1-min (Fig. 8(a)) and 3-min (Fig. 8(b)) irradiation times [49]. After a 5-min irradiation time, Ru particles have generally been transformed into single crystals with the associated disappearance of twins. The crystalline structure and the exposed facets of the single crystal NPs can be indexed, as shown in Fig. 8(c). On the basis of the Wulff construction, the exposed facets of most Ru NPs are approximately terminated by these planes (e.g., {012}, {112}, {111}, {100}, {101}, and {002}). In addition, the facets of Ru NPs in contact with CNTs can also be identified.

2.4. Monitoring dynamic processes in the TEM

Electron microscopy has become crucial in catalysis chemistry: it does not only provide real-space images at the atomic level of the defects and surface structures that largely control the performance of solid catalysts, but it is also widely used for in situ heating experiments [66–68], for controlled electron beam irradiation [47,69–71], for manipulation using special setups in EM labs [72,73], or for introducing gas to directly observe the microstructural evolution and active sites of catalysts under dynamic reaction conditions [74–76]. This leads to a better understanding of the structure–performance

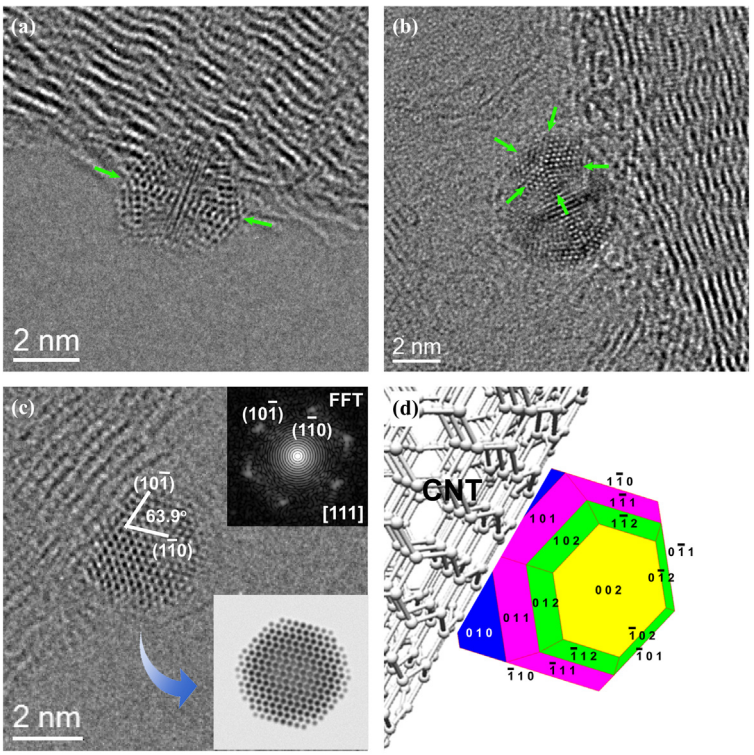

Fig. 8. (Color online.) Typical HRTEM images of Ru/CNTs—1 min (a), Ru/CNTs—3 min (b), and Ru/CNTs—5 min (c) samples. The corresponding shape of the nanoparticle in (c) with indexed faceting configurations is shown in (d). Insets in (c) are the local Fast Fourier Transform (FFT) of the HRTEM image and a simulated HRTEM image matching satisfactorily its experimental counterpart. Reprinted with permission from [49], copyright (2011) The Royal Society of Chemistry.

relationship and consequently to the optimization of heterogeneous catalysts as well as to the design of new structures with desired properties. Fig. 9 displays the response of a single nanocrystalline particle under electron beam irradiation [47]. The particle exhibits dynamical structural changes, while still maintaining its long-range order. A change in the particle shape accompanies the structural fluctuation (Fig. 9(a)–(e)), which was reconstructed as shown in Fig. 9(f)–(j). The surface exposure dynamically changed under the beam irradiation with, for example, an emergence and disappearance of {110}. The FFT (Fig. 9(k)–(o)) reveals that the orientation of the particle has been changing with beam irradiation due to a varying acute angle of {111} and {200}. Such studies complement the most useful and extensive investigations on model systems that usually exclude structural dynamics from their observation techniques [47].

Another example is the monitoring of the redox behavior of TiO_2/SBA-15 supported V_xO_y catalyst using an electron beam [69]. The electron beam can boost further oxidation from an amorphous lower-oxidation-stage vanadia to maximal V_2O_5 with an expense of oxygen from its support of TiO_2 to be reduced, which has been studied by in situ EELS. Fig. 10 shows a normalized EELS series of the sample under the electron irradiation, displaying that the existence of O K, white line Ti L_{III}/L_{II} and V L_{III}/L_{II} edges. With electron irradiation, a gradual peak broadening for Ti L_{III}/L_{II} edges is observed by comparing the initial EELS A with final EELS L (Fig. 10(b)), indicating a lowered coordination of titanium, which illustrates a reduction process of TiO_2 to TiO_{2-x}. Meanwhile, the peaks of V L_{III}/L_{II} edges shifted to higher energy loss, and the relative ratio of V L_{III}/L_{II} decreases gradually (Fig. 10(c)), which shows an oxidation process of V_xO_y. This study highlights the high potential of in situ EELS. It actually gives information on the electronic structure of catalysts monitored in real time under the influence of the incident electron beam and could thus provide hints for understanding the redox chemistry between catalysts and their support in heterogeneous catalytic systems.

The limitations imposed by the beam–catalyst interaction must be pointed out, although some information about the interaction between supported phases and supports can be obtained by controlling electron beam irradiation. Usually, the electron beam effects should be avoided in order to get the real structural information about catalysts, especially in the case of electron-beam-sensitive ones [23].

3. Summary

In this review, we have described some examples that highlight the importance of TEM in the field of heterogeneous catalysis. The TEM instrument has evolved from a magnifying instrument towards a versatile research tool for revealing morphological, crystallographic, compositional, electronic, magnetic information of solid catalysts at the sub-angstrom scale.

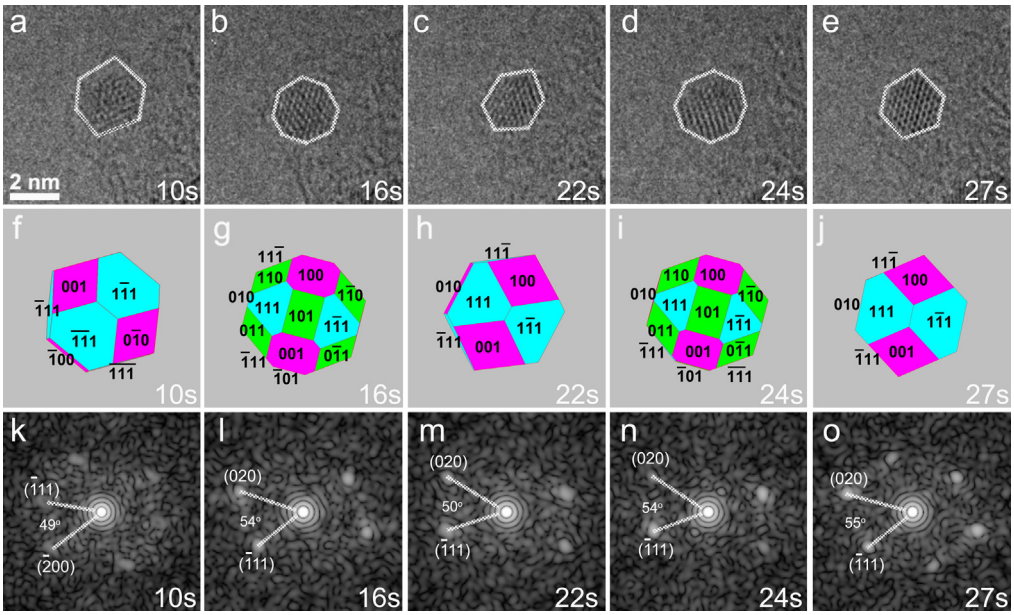

Fig. 9. (Color online.) Series of HRTEM images (a)–(e) with the corresponding particle shapes (f)–(j) and FFT patterns (k)–(o) of one small Au particle at various observation times. Electron doses: (a) 22×10^6, (b) 35.2×10^6, (c) 48.4×10^6, (d) 52.8×10^6, (e) 59.4×10^6 $e^- nm^{-2}$. Reprinted with permission from [47], copyright (2011) Wiley-VCH Verlag GmbH & Co. KGaA, Weinheim, Germany.

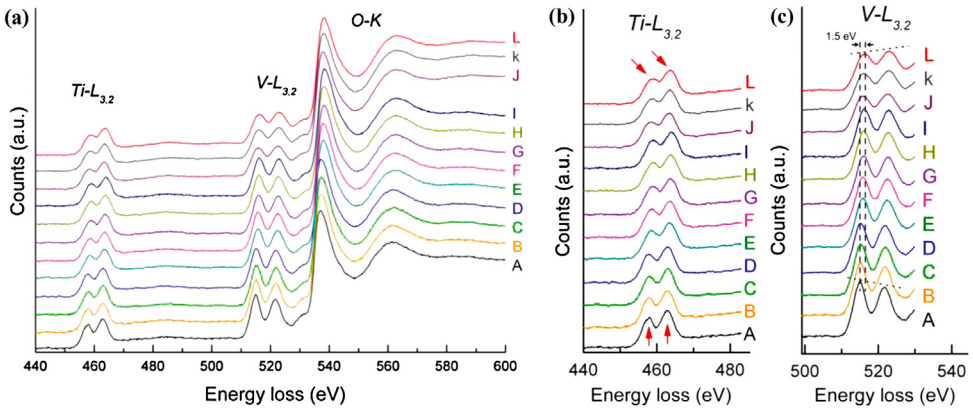

Fig. 10. (Color online.) In situ normalized EELS series (after background removal and deconvolution) (a) of the sample under the electron irradiation. Electron doses and irradiation time: A, 3×10^4 e^-/nm^2, 0 min; B, 520×10^4 e^-/nm^2, 3 min; C, 100×10^5 e^-/nm^2, 6 min; D, 180×10^5 e^-/nm^2, 10.5 min; E, 260×10^5 e^-/nm^2, 15 min; F, 290×10^5 e^-/nm^2, 16.5 min; G, 370×10^5 e^-/nm^2, 21 min; H, 420×10^5 e^-/nm^2, 24 min; I, 470×10^5 e^-/nm^2, 27 min; J, 760×10^5 e^-/nm^2, 30 min; K, 1020×10^5 e^-/nm^2, 31.5 min; L, 1280×10^5 e^-/nm^2, 3 min. (b), (c) Local enlargements of the Ti-edges and V-edges in (a). Reprinted with permission from [69], copyright (2011) The American Chemical Society.

Now, we are living in a historic era for electron microscopy, with the development of spherical aberration correctors, monochromators, tomography, holography, cryo-TEM, environmental-TEM, low-voltage TEM, and some special specimen holders for in situ dynamic experiments. Furthermore, the development of EM has been from 2D via 3D to 4D [77–79], which can yield information in four distinct ways: in real space, in reciprocal space, in energy space, and in the time domain [80]. Such progress will open a unique window to investigate the structural, chemical and electronic information of complex catalysts. In addition, the dynamic in-situ EM can reveal more important information to explore the catalysts under working conditions. All of these progresses can definitely assist us to establish the synthesis–structure–property relationship, and to design and fabricate new catalysts with the desired performances.

Acknowledgements

We gratefully acknowledge the financial support provided by the IMR SYNL-T.S. Kê Research Fellowship, NSFC of China (21203215, 21133010, 51221264, 21261160487), MOST (2011CBA00504), “Strategic Priority Research Program” of the Chinese Academy of Sciences (Grant No. XDA09030103), and the China Postdoctoral Science Foundation (2012M520652).

References

[1] R. Schlogl, The role of chemistry in the energy challenge, ChemSusChem 3 (2010) 209–222.
[2] G.A. Somorjai, B. Chaudret, P. Serp, K. Philippot, Nanomaterials in Catalysis, John Wiley & Sons, 2012.
[3] G. Van Tendeloo, S. Bals, S. Van Aert, J. Verbeeck, D. Van Dyck, Advanced electron microscopy for advanced materials, Adv. Mater. 24 (2012) 5655–5675.
[4] W. Zhou, I.E. Wachs, C.J. Kiely, Nanostructural and chemical characterization of supported metal oxide catalysts by aberration corrected analytical electron microscopy, Curr. Opin. Solid State Mater. Sci. 16 (2012) 10–22.
[5] J.Y. Liu, Advanced electron microscopy of metal–support interactions in supported metal catalysts, ChemCatChem 3 (2011) 934–948.
[6] J.M. Thomas, P.A. Midgley, The merits of static and dynamic high-resolution electron microscopy (HREM) for the study of solid catalysts, ChemCatChem 2 (2010) 783–798.
[7] J.C. Yang, M.W. Small, R.V. Grieshaber, R.G. Nuzzo, Recent developments and applications of electron microscopy to heterogeneous catalysis, Chem. Soc. Rev. 41 (2012) 8179–8194.
[8] S.I. Sanchez, M.W. Small, S. Sivaramakrishnan, J.G. Wen, J.M. Zuo, R.G. Nuzzo, Visualizing materials chemistry at atomic resolution, Anal. Chem. 82 (2010) 2599–2607.
[9] H.L. Xin, D.A. Muller, Aberration-corrected ADF-STEM depth sectioning and prospects for reliable 3D imaging in S/TEM, J. Electron Microsc. 58 (2009) 157–165.
[10] H. Friedrich, P.E. de Jongh, A.J. Verkleij, K.P. de Jong, Electron tomography for heterogeneous catalysts and related nanostructured materials, Chem. Rev. 109 (2009) 1613–1629.
[11] J.Y. Liu, Scanning transmission electron microscopy and its application to the study of nanoparticles and nanoparticle systems, J. Electron Microsc. 54 (2005) 251–278.
[12] P.L. Gai, J.J. Calvino, Electron microscopy in the catalysis of alkane oxidation, environmental control, and alternative energy sources, in: Annual Review of Materials Research, Annual Reviews, Palo Alto, 2005, pp. 465–504.
[13] J.M. Thomas, P.L. Gal, Electron microscopy and the materials chemistry of solid catalysts, in: B.C. Gates, H. Knozinger (Eds.), Advances in Catalysis, vol. 48, Elsevier Academic Press Inc., San Diego, 2004, pp. 171–227.
[14] J.Y. Liu, Advanced electron microscopy characterization of nanostructured heterogeneous catalysts, Microsc. Microanal. 10 (2004) 55–76.
[15] J.M. Thomas, O. Terasaki, P.L. Gai, W.Z. Zhou, J. Gonzalez-Calbet, Structural elucidation of microporous and mesoporous catalysts and molecular sieves by high-resolution electron microscopy, Acc. Chem. Res. 34 (2001) 583–594.
[16] P.L. Gai, Developments of electron microscopy methods in the study of catalysts, Curr. Opin. Solid State Mater. Sci. 5 (2001) 371–380.
[17] S. Bernal, R.T. Baker, A. Burrows, J.J. Calvino, C.J. Kiely, C. Lopez-Cartes, J.A. Perez-Omil, J.M. Rodriguez-Izquierdo, Structure of highly dispersed metals and oxides: exploring the capabilities of high-resolution electron microscopy, Surf. Interface Anal. 29 (2000) 411–421.
[18] D.S. Su, Electron tomography: from 3D statics to 4D dynamics, Angew. Chem., Int. Ed. Engl. 49 (2010) 9569–9571.
[19] N. de Jonge, F.M. Ross, Electron microscopy of specimens in liquid, Nat. Nanotechnol. 6 (2011) 695–704.
[20] X.Z. Yu, Y. Onose, N. Kanazawa, J.H. Park, J.H. Han, Y. Matsui, N. Nagaosa, Y. Tokura, Real-space observation of a two-dimensional skyrmion crystal, Nature 465 (2010) 901–904.
[21] L. Shao, B. Zhang, W. Zhang, S.Y. Hong, R. Schlögl, D.S. Su, The role of palladium dynamics in the surface catalysis of coupling reactions, Angew. Chem., Int. Ed. Engl. 52 (2013) 2114–2117.
[22] B. Zhang, D.S. Su, Transmission electron microscopy and the science of carbon nanomaterials, Small (2013), http://dx.doi.org/10.1002/smll.201301303.
[23] G. Van Tendeloo, D. Van Dyck, S.J. Pennycook, Handbook of Nanoscopy, Wiley, 2012.
[24] D.S. Su, Special issue: advanced electron microscopy for catalysis, ChemCatChem 3 (2011) 919–920.
[25] D.S. Su, Special issue: advanced electron microscopy for catalysis, ChemCatChem 5 (2013) 2543–2545.
[26] J.M. Thomas, C. Ducati, R. Leary, P.A. Midgley, Some turning points in the chemical electron microscopic study of heterogeneous catalysts, ChemCatChem 5 (2013) 2560–2579.
[27] J.M. Thomas, R. Raja, The advantages and future potential of single-site heterogeneous catalysts, Top. Catal. 40 (2006) 3–17.
[28] B.S. Zhang, Y.J. Yi, W. Zhang, C.H. Liang, D.S. Su, Electron microscopy investigation of the microstructure of unsupported Ni–Mo–W sulfide, Mater. Charact. 62 (2011) 684–690.
[29] L.D. Shao, B.S. Zhang, W. Zhang, S.Y. Hong, R. Schlogl, D.S. Su, The role of palladium dynamics in the surface catalysis of coupling reactions, Angew. Chem., Int. Ed. Engl. 52 (2013) 2114–2117.
[30] G.A. Botton, S. Lazar, C. Dwyer, Elemental mapping at the atomic scale using low accelerating voltages, Ultramicroscopy 110 (2010) 926–934.
[31] B. Zhang, W. Zhang, L. Shao, D.S. Su, Optimum energy-dispersive X-ray spectroscopy elemental mapping for advanced catalytic materials, ChemCatChem 5 (2013) 2586–2590.
[32] L.D. Shao, B.S. Zhang, W. Zhang, D. Teschner, F. Girgsdies, R. Schlogl, D.S. Su, Improved selectivity by stabilizing and exposing active phases on supported Pd nanoparticles in acetylene-selective hydrogenation, Eur. J. Chem. 18 (2012) 14962–14966.
[33] L.D. Li, B.S. Zhang, E. Kunkes, K. Fottinger, M. Armbruster, D.S. Su, W. Wei, R. Schlogl, M. Behrens, Ga–Pd/Ga_2O_3 catalysts: the role of gallia polymorphs, intermetallic compounds, and pretreatment conditions on selectivity and stability in different reactions, ChemCatChem 4 (2012) 1764–1775.
[34] D. Wang, A. Villa, P. Spontoni, D.S. Su, L. Prati, In situ formation of Au–Pd bimetallic active sites promoting the physically mixed monometallic catalysts in the liquid-phase oxidation of alcohols, Eur. J. Chem. 16 (2010) 10007–10013.
[35] X.C. Zhao, Q. Zhang, B.S. Zhang, C.M. Chen, A.Q. Wang, T. Zhang, D.S. Su, Dual-heteroatom-modified ordered mesoporous carbon: Hydrothermal functionalization, structure, and its electrochemical performance, J. Mater. Chem. 22 (2012) 4963–4969.
[36] C. Chen, J. Zhang, B. Zhang, C. Yu, F. Peng, D. Su, Revealing the enhanced catalytic activity of nitrogen-doped carbon nanotubes for oxidative dehydrogenation of propane, Chem. Commun. 49 (2013) 8151–8153.
[37] K. Suenaga, M. Koshino, Atom-by-atom spectroscopy at graphene edge, Nature 468 (2010) 1088–1090.
[38] C. Colliex, From electron energy-loss spectroscopy to multi-dimensional and multi-signal electron microscopy, J. Electron Microsc. 60 (2011) S161–S171.
[39] S. Trasobares, M. Lopez-Haro, M. Kociak, K. March, F. de La Pena, J.A. Perez-Omil, J.J. Calvino, N.R. Lugg, A.J. D'Alfonso, L.J. Allen, C. Colliex, Chemical imaging at atomic resolution as a technique to refine the local structure of nanocrystals, Angew. Chem., Int. Ed. Engl. 50 (2011) 868–872.
[40] C.P. Ewels, A. Gloter, T. Minea, B. Bouchet-Fabre, S. Point, C. Colliex, Influence of Fe/Cr on nitrogen doped carbon nanotube growth, Eur. Phys. J. Appl. Phys. 42 (2008) 247–250.
[41] N.Y. Jin-Phillipp, C.T. Koch, P.A. van Aken, Toward quantitative core-loss EFTEM tomography, Ultramicroscopy 111 (2011) 1255–1261.
[42] D.L. Wang, H.L.L. Xin, R. Hovden, H.S. Wang, Y.C. Yu, D.A. Muller, F.J. DiSalvo, H.D. Abruna, Structurally ordered intermetallic platinum–cobalt core–shell nanoparticles with enhanced activity and stability as oxygen reduction electrocatalysts, Nat. Mater. 12 (2013) 81–87.
[43] X.C. Zhao, Q. Zhang, B.S. Zhang, C.M. Chen, J.M. Xu, A.Q. Wang, D.S. Su, T. Zhang, Decorated resol derived mesoporous carbon: highly ordered microstructure, rich boron incorporation, and excellent electrochemical capacitance, RSC Adv. 3 (2013) 3578–3584.
[44] X. Bao, M. Muhler, B. Pettinger, R. Schlogl, G. Ertl, On the nature of the active state of silver during catalytic-oxidation of methanol, Catal. Lett. 22 (1993) 215–225.
[45] X. Bao, M. Muhler, R. Schlogl, G. Ertl, Oxidative coupling of methane on silver catalysts, Catal. Lett. 32 (1995) 185–194.

[46] D.S. Su, T. Jacob, T.W. Hansen, D. Wang, R. Schlogl, B. Freitag, S. Kujawa, Surface chemistry of Ag particles: Identification of oxide species by aberration-corrected TEM and by DFT calculations, Angew. Chem., Int. Ed. Engl. 47 (2008) 5005–5008.
[47] B.S. Zhang, D. Wang, W. Zhang, D.S. Su, R. Schlogl, Structural dynamics of low-symmetry Au nanoparticles stimulated by electron irradiation, Eur. J. Chem. 17 (2011) 12877–12881.
[48] B.S. Zhang, W. Zhang, D.S. Su, Towards a more accurate particle size distribution of supported catalyst by using HAADF–STEM, ChemCatChem 3 (2011) 965–968.
[49] B.S. Zhang, X.J. Ni, W. Zhang, L.D. Shao, Q. Zhang, F. Girgsdies, C.H. Liang, R. Schlogl, D.S. Su, Structural rearrangements of Ru nanoparticles supported on carbon nanotubes under microwave irradiation, Chem. Commun. 47 (2011) 10716–10718.
[50] B.T. Qiao, A.Q. Wang, X.F. Yang, L.F. Allard, Z. Jiang, Y.T. Cui, J.Y. Liu, J. Li, T. Zhang, Single-atom catalysis of CO oxidation using Pt_1/FeO_x, Nat. Chem. 3 (2011) 634–641.
[51] B.S. Zhang, W. Zhang, D.S. Su, Analysis of particle size distribution of supported catalyst by HAADF–STEM, Microsc. Anal. 26 (2012) 15–20.
[52] K. Arve, H. Kannisto, H.H. Ingelsten, K. Eranen, M. Skoglundh, D.Y. Murzin, Did chemisorption become an obsolete method with advent of TEM? Comparison of mean particle size and distribution of silver on alumina, Catal. Lett. 141 (2011) 665–669.
[53] J.P. Tessonnier, O. Ersen, G. Weinberg, C. Pham-Huu, D.S. Su, R. Schlogl, Selective deposition of metal nanoparticles inside or outside multiwalled carbon nanotubes, ACS Nano 3 (2009) 2081–2089.
[54] E.P.W. Ward, T.J.V. Yates, J.J. Fernandez, D.E.W. Vaughan, P.A. Midgley, Three-dimensional nanoparticle distribution and local curvature of heterogeneous catalysts revealed by electron tomography, J. Phys. Chem. C 111 (2007) 11501–11505.
[55] J.C. Hernandez-Garrido, K. Yoshida, P.L. Gai, E.D. Boyes, C.H. Christensen, P.A. Midgley, The location of gold nanoparticles on titania: A study by high resolution aberration-corrected electron microscopy and 3D electron tomography, Catal. Today 160 (2011) 165–169.
[56] R. Leary, P.A. Midgley, J.M. Thomas, Recent advances in the application of electron tomography to materials chemistry, Acc. Chem. Res. 45 (2012) 1782–1791.
[57] B. Goris, S. Bals, W. Van den Broek, E. Carbo-Argibay, S. Gomez-Grana, L.M. Liz-Marzan, G. Van Tendeloo, Atomic-scale determination of surface facets in gold nanorods, Nat. Mater. 11 (2012) 930–935.
[58] S. Bals, M. Casavola, M.A. van Huis, S. Van Aert, K.J. Batenburg, G. Van Tendeloo, D. Vanmaekelbergh, Three-dimensional atomic imaging of colloidal core–shell nanocrystals, Nano Lett. 11 (2011) 3420–3424.
[59] C.-C. Chen, C. Zhu, E.R. White, C.-Y. Chiu, M.C. Scott, B.C. Regan, L.D. Marks, Y. Huang, J. Miao, Three-dimensional imaging of dislocations in a nanoparticle at atomic resolution, Nature 496 (2013) 74–77.
[60] C.M. Chen, Q. Zhang, C.H. Huang, X.C. Zhao, B.S. Zhang, Q.Q. Kong, M.Z. Wang, Y.G. Yang, R. Cai, D.S. Su, Macroporous 'bubble' graphene film via template-directed ordered-assembly for high rate supercapacitors, Chem. Commun. 48 (2012) 7149–7151.
[61] C.-C. Chen, C. Zhu, E.R. White, C.-Y. Chiu, M.C. Scott, B.C. Regan, L.D. Marks, Y. Huang, J. Miao, Three-dimensional imaging of dislocations in a nanoparticle at atomic resolution, Nature 496 (2013) 74–77.
[62] M.C. Scott, C.C. Chen, M. Mecklenburg, C. Zhu, R. Xu, P. Ercius, U. Dahmen, B.C. Regan, J.W. Miao, Electron tomography at 2.4-angstrom resolution, Nature 483 (2012) 444–U491.
[63] S. Van Aert, K.J. Batenburg, M.D. Rossell, R. Erni, G. Van Tendeloo, Three-dimensional atomic imaging of crystalline nanoparticles, Nature 470 (2011) 374–377.
[64] B. Zhang, D.S. Su, Electron tomography: three-dimensional imaging of real crystal structures at atomic resolution, Angew. Chem., Int. Ed. Engl. 52 (2013) 8504–8506.
[65] K. Philippot, P. Serp, Concepts in nanocatalysis, in: Nanomaterials in Catalysis, Wiley-VCH Verlag GmbH & Co. KGaA, 2013, pp. 1–54.
[66] Z.L. Zhang, D.S. Su, Behaviour of TEM metal grids during in-situ heating experiments, Ultramicroscopy 109 (2009) 766–774.
[67] J. Zhang, J.O. Muller, W.Q. Zheng, D. Wang, D.S. Su, R. Schlogl, Individual Fe–Co alloy nanoparticles on carbon nanotubes: Structural and catalytic properties, Nano Lett. 8 (2008) 2738–2743.
[68] S.R. Challa, A.T. Delariva, T.W. Hansen, S. Helveg, J. Sehested, P.L. Hansen, F. Garzon, A.K. Datye, Relating rates of catalyst sintering to the disappearance of individual nanoparticles during Ostwald ripening, J. Am. Chem. Soc. 133 (2011) 20672–20675.
[69] W. Zhang, B.S. Zhang, T. Wolfram, L.D. Shao, R. Schlogl, D.S. Su, Probing a redox behavior of TiO_2/SBA-15 supported VxOy catalyst using an electron beam in a 200 kV transmission electron microscope, J. Phys. Chem. C 115 (2011) 20550–20554.
[70] T.W. Chamberlain, J.C. Meyer, J. Biskupek, J. Leschner, A. Santana, N.A. Besley, E. Bichoutskaia, U. Kaiser, A.N. Khlobystov, Reactions of the inner surface of carbon nanotubes and nanoprotrusion processes imaged at the atomic scale, Nat. Chem. 3 (2011) 732–737.
[71] B. Zhang, L. Shao, W. Zhang, D.S. Su, Clothing carbon nanotubes with palladium rings: constructing carbon–metal hybrid nanostructures under electron-beam irradiation, ChemCatChem 5 (2013) 2581–2585.
[72] S. Chenna, P.A. Crozier, Operando transmission electron microscopy: a technique for detection of catalysis using electron energy-loss spectroscopy in the transmission electron microscope, ACS Catal. 2 (2012) 2395–2402.
[73] C. Jin, K. Suenaga, S. Iijima, How does a carbon nanotube grow? An in situ investigation on the cap evolution, ACS Nano 2 (2008) 1275–1279.
[74] P.L. Hansen, J.B. Wagner, S. Helveg, J.R. Rostrup-Nielsen, B.S. Clausen, H. Topsøe, Atom-resolved imaging of dynamic shape changes in supported copper nanocrystals, Science 295 (2002) 2053–2055.
[75] H. Yoshida, Y. Kuwauchi, J.R. Jinschek, K.J. Sun, S. Tanaka, M. Kohyama, S. Shimada, M. Haruta, S. Takeda, Visualizing gas molecules interacting with supported nanoparticulate catalysts at reaction conditions, Science 335 (2012) 317–319.
[76] P.L. Gai, E.D. Boyes, S. Helveg, P.L. Hansen, S. Giorgio, C.R. Henry, Atomic-resolution environmental transmission electron microscopy for probing gas–solid reactions in heterogeneous catalysis, Mater. Res. Soc. Bull. 32 (2007) 1044–1050.
[77] O.H. Kwon, A.H. Zewail, 4D electron tomography, Science 328 (2010) 1668–1673.
[78] A.H. Zewail, Four-dimensional electron microscopy, Science 328 (2010) 187–193.
[79] R.M. van der Veen, O.-H. Kwon, A. Tissot, A. Hauser, A.H. Zewail, Single-nanoparticle phase transitions visualized by four-dimensional electron microscopy, Nat. Chem. 5 (2013) 395–402.
[80] A.H. Zewail, 4D Electron Microscopy: Imaging in Space and Time, World Scientific, 2009.